Original Article

Institution of MECHANICAL ENGINEERS

Journal of ENGINEERING TRIBOLOGY

Tribological analyses of a new optimized gearbox biodegradable lubricant blended with reduced graphene oxide nanoparticles

Proc IMechE Part J:
J Engineering Tribology
1–15

DOI: 10.1177/1350650120925590
journals.sagepub.com/home/pij
SAGE

Shubrajit Bhaumik[1], M Kamaraj[2] and Viorel Paleu[3]

Abstract

The current work aims to develop a biodegradable lubricant by adding different volume percentages of cashew nut shell liquid (CNSL) in neat castor oil (NCO) and investigating its possibility as replacement to non-biodegradable mineral oil (commercial mineral oil) in industrial applications. The blend exhibiting better tribological properties was additived with different weight percentages of reduced graphene oxide (r-GO) nano-platelets and further tribological tests were performed. The performance of 40%CNSL+NCO was 45.8% better than commercial mineral oil, and with the addition of the 0.5% r-GO in the blend, the performance was improved by 61.7% than the commercial mineral oil. Finally, the novel biodegradable mixture blended with nanoparticles was employed as a lubricant in a gearbox, proving the superiority of the biodegradable lubricant over the commercial mineral oil.

Keywords

Biodegradable lubricant, reduced graphene oxide nanoparticles, wear, gearboxes, nanolubricants, tribology

Date received: 24 January 2020; accepted: 18 April 2020

Introduction

An invaluable role is played by lubricants in reducing wear and friction of mechanical components in the industry. The rationale behind numerous companies advancing in the research and development of lubrication enhancement arrives from a common resolution that tribological-related hindrances during the running of machines cause severe damage to the workpieces as well as the machining equipments.[1] The usage of lubricants is not constrained to a particular field, as lubrication is indispensable in all mechanical instruments and rotating machineries in automotive, industrial and marine applications in order to mitigate the effects of power loss and maintain a judicious use of resources.[2] As far as curbing the wastage of resources is concerned, management and sustentation of energy, materials and resources is steadily becoming an imminent global issue. It has been reported that 85%–90% of the total produced lubricants in the world originate from non-renewable mineral oil sources.[3] With these aspects taken into consideration, researchers have shifted their interest towards the new emerging areas for developing biodegradable products, the most prominent being known as 'Go Green Concept'. Apart from the approaches of minimising energy dissipation, improving service lifetime and component compatibility, green tribology also deals with sustainability and life cycle assessment (LCA) of the related components.[4] Encompassing the latter two facets of the field as mentioned above, biodegradable lubrication is the most principal element to be taken into consideration; yearly it is being reported that tons of lubricant wastes are released to the environment across the world[5] Thus, the attention has now transposed to the usage of ecologically benign lubricants to diminish the exploitation of petroleum-based lubricant oils dominating in the industry. Gear boxes are important part of any machinery, being employed in many fields such as cement, power, and steel industries. In several

[1]Tribology and Surface Interaction Research Laboratory, Department of Mechanical Engineering, SRM Institute of Science and Technology, Kattankulathur, India
[2]Metallurgy and Materials Engineering, Indian Institute of Technology Madras, Chennai, India
[3]Mechanical Engineering, Mechatronics and Robotics Department, Gheorghe Asachi Technical University of Iasi, Iasi, Romania

Corresponding author:
Shubrajit Bhaumik, SRM Institute of Science and Technology, Kattankulathur 603203, India.
Email: shubrajb@srmist.edu.in

applications such as conveyor belts, rolling mills, kilns, etc., these gear boxes are directly responsible of smooth plant operation. Usually, the gear boxes need to be lubricated, and hence lubricants form an essential mechanical element in industries. As various types of lubricating oils such as mineral oils and synthetic oils are available in the market, vegetable oils have now taken importance due to their several advantages over the former mentioned oils. Petroleum-based oils offer lubricity against their high cost, toxicity and non-biodegradable nature, whereas vegetable-based lubricating oils offer biodegradability, high viscosity indices, low volatility, low toxicity, high flash points, low production costs, easy additive combinations and low environmental pollution,[6–10] becoming an attractive alternative to petroleum oils.[11] This has led the researchers to propose vegetable oils as lubricants.[12–30] The distinctive feature of vegetable oil is its structure which comprises of polar groups and long chain fatty acids. This makes vegetable oils befitting for lubrication in different regimes.[31] Promising work has been reported using many vegetable oils such as jatropha oil, jojoba oil, mahua oil, rapeseed oil etc., which have shown reasonable results as compared to commercially available mineral oils.[12,32–39] Cashew nuts are grown in surplus in India, and thus a vegetable oil can be easily obtained[40] from cashew nuts. Cashew nut shell liquid (CNSL) is produced while processing of cashews which is produced before cardanol and thus can be considered as one of the natural substitutes to the mineral oils used in industry.[41] CNSL is a distinguishable reddish brown low viscous liquid extracted from the shells of cashew nuts. The main component of CNSL is anacardic acid (78%), which is a form of fatty acid chain and minor quantities of 2-methyl cardol, cardanol and polymeric material.[42] As reported in the literature, CNSL seems to possess better combustion, performance and emission characteristics, which corroborates its usage as engine oils.[43] Another example of an excellent vegetable oil which can be used as a sustainable lubricant, as it allocates significantly comparable results with commercial mineral oil, is castor oil.[44–46] The versatility of castor oil due to its manifold edge in the industrial and maintenance applications cannot be underestimated, as it upholds several factors such as high biodegradability, natural lubricity, excellent viscosity features and low toxicity. Although it is perquisite to use vegetable oils for several roles in the lubrication industry, not all vegetable oils are sufficient for retaining equivalent chemical, physical as well as tribological properties (low friction coefficient and diminished wear intensity, high pressure resistance, high viscosity index etc.). Thus, the approach of blending is taken into consideration. This technique inspects the base oils' interaction with the tribo pairs in order to set up lubricating contact surfaces for a range of ambient conditions. Both castor oil as well as cashew nut shell liquid possess assertive characteristics pertaining to their chemical composition and molecular arrangements.[47,48] Both of them possess similar densities, good biodegradability, good miscibility, enhanced viscosity features and conceivable response in hydrodynamic as well as boundary lubrication regime.[49,50] Despite vegetable oils having several beneficial characteristics, their oxidation is a major problem, which affects their performance. Thus, researchers have been studying the effects of friction modifiers and additives in industrial lubricants.[51–59] Additives are added in the lubricants as packages which are used for performance enhancement of the lubricant. Out of all the kinds of additives, solid additives are commonly used due to their applications in high contact loads and low sliding speeds as they prevent lubricant starvation at tribo pairs. Literature proposes graphene as an effective solid lubricant[60–63] in industrial oils as it is chemically inert, possesses high extreme strength property, has an ability to shear effortlessly on its sliding surfaces and also slows down the corrosive and oxidative processes that causes majority of damages on the surface.[64] However, due to significant agglomeration within the lubricant in graphene, the applications are limited.[65] Covalent functionalization of graphene oxide paves way for the formation of reduced graphene oxide (r-GO) which in turn introduces a polar group and straight hydrocarbon tail on the surface of graphene oxide. This characteristic of r-GO can be unique property for vegetable oil lubricants, as it substantially complements anti-wear and antifriction properties. Monolayer r-GO sheet as efficient additives in water-based lubricants was reported by Kinoshita et al.[66] Zhang et al.[67] dispersed magnetic r-GO/Fe_3O_4 composite in polyalfaolefin (PAO 6) oils and investigated the friction reduction capability of these r-GO composites. It was reported that the presence of r-GO/Fe_3O_4 particles improved the antiwear properties of PAO 6.

Additionally, it has been concluded by several researchers[68–73] that supplementary to shape, size and concentration of friction modifiers, properties like shear modulus, specific surface area and elastic modulus are responsible for the reduction of friction. The authors have previously worked upon the analysis of tribological properties of various friction modifiers added to castor oil samples and compared the tribological results with the commercial non-biodegradable mineral oil, emphasizing the possibility of using castor oil as an alternative to mineral oils.[44–46] This work aims to obtain a new biodegradable lubricant as a plausible replacement for the commercial non-biodegradable oils. The optimization of the percentage of CNSL, neat castor oil (NCO) and r-GO friction modifier in a new biodegradable lubricating mixture was realized by the results of tests on a four-ball machine and post-processing techniques of the worn surfaces of balls.

Materials and methods

Preparation of NCO/ CNSL/r-GO blend

NCO, CNSL, and commercial mineral oil without any further processing and treatment were procured from a local market (Chennai, India) and have been chosen as the experimental base oils. Laboratory analysis of commercial mineral oil (CMO) revealed the presence of phosphorus (4 ppm) and sulphur (4977 ppm). NCO and CNSL have been chosen, as they are readily accessible in India; NCO has a high viscosity (242.81 cSt @ 40 °C) and CNSL has a high biodegradability. The lubricant blend was prepared by adding CNSL into NCO on a volume percentage basis (10%, 20%, 30%, 40%, 50%, 60%, and 70%). The prepared oil had been thoroughly agitated with mechanical stirrer before conducting each experiment. Both oils, NCO and CNSL, had been characterized in order to comprehend the amount of fatty acids content as stated in Tables 1 and 2. The procured reduced graphene oxide (M/s United Nanotech P Ltd, India) on different weight % basis (0.1%, 0.5%, 1% and 2%) was added to the least frictional coefficient, yielding blend ratio of NCO and CNSL. The suspensions were first stirred using a magnetic stirrer for 120 min followed by sonication (probe-sonicator for 45 min). The fatty acid content of NCO and CNSL was determined using a gas chromatography as shown in Table 1.

Table 1. Spectrometric results of NCO.

Parameters	Units	NCO	CNSL
Saturated fatty acid	g/100 g	43.10	31.1
Mono unsaturated fatty acid	g/100 g	54.85	68.9
Poly-unsaturated fatty acid	g/100 g	1.31	<0.1

NCO: neat castor oil; CNSL: cashew nut shell liquid.

Measuring viscosity, flash point and fire point

Redwood viscometer (Make: Abels) and Cleveland open cup apparatus (Make: Abels) were used to determine the physio-chemical properties of the oil samples.

Determination of anti-wear property

Four-ball test rig was used in order to determine the anti-wear (AW) properties (ASTM 4172 – axial load: 392 N, speed: 1200 r/min, time: 3600 s, temperature: 75 °C).[44] The balls used throughout the tests are AISI 52100 with 12.7 mm diameter and 60 HRc. The three stationary balls in the testing device were held steadfast and the fourth ball rotated on top. The results presented in this paper are the average value of three identically carried out experiments. Wear scar diameters (WSD) were measured using an optical microscope (Model: Olympus, BX41M).

Determining the extreme pressure property

The extreme pressure (EP) property was calculated for both samples: with optimum blend the ratio of CNSL in NCO, and with optimum r-GO concentration in the optimum blend of CNSL–NCO. The three stationary balls were worked upon a fourth ball on top at a speed of 1760 r/min for 10 s at various loads till welding load was determined according to ASTM D 2783. The following terminologies can be considered of interest: Hertz diameter (D′), Hertz line, compensation line,

Table 2. Physico-chemical properties of the oil samples.

Oil Samples	Viscosity at 40 °C (cSt)	Viscosity at 100 °C (cSt)	Flash point (°C)	Fire point (°C)
CMO	559.60	48.80	245	250
NCO	242.81	18.10	270	275
CNSL	65.03	8.04	230	242
NCO + 10% CNSL	242.16	19.16	240	250
NCO+20% CNSL	238.33	19.54	240	250
NCO+30% CNSL	222.31	18.9	242	256
NCO + 40% CNSL	215.61	17.99	250	260
NCO + 50% CNSL	209.11	17.36	250	260
NCO + 60% CNSL	201.89	17.19	250	260
NCO + 70% CNSL	191.13	14.12	247	253
0.1% r-GO + 40% CNSL + NCO	131.32	14.31	246	251
0.5% r-GO + 40% CNSL + NCO	198.58	16.78	265	275
1% r-GO + 40% CNSL + NCO	205.8	16.4	260	270
2% r-GO + 40% CNSL + NCO	208.26	16.67	265	275

NCO: neat castor oil; CNSL: cashew nut shell liquid; r-GO: reduced graphene oxide.

initial seizure load (ISL), last non-seizure load (LNSL), and weld load (WL).

Analyzing the tested ball surfaces

In order to measure the surface roughness (SR), a 3D Taylor Hobson CCI MP-HS profilometer was used. In order to understand the severity of wear occurring during the tribotests, the surfaces of the lower balls after tribo test were observed using a scanning electron microscopy (SEM), and the deposition/formation of various elements were analyzed using an energy dispersive system (EDS). The average roughness, Ra and the mean square roughness, Rq, were determined along the wear scar of tested balls using a three-dimensional profilometer (Make: Taylor Hobson).

Results

The results of the present investigation focus on the optimization of the percentage of CNSL, NCO and r-GO friction modifier in the new biodegradable mixture. The performances of the new biodegradable oil mixture are compared against those of a commercial mineral oil.

Viscosity, flash point and fire point

As it can be seen from Table 2, the viscosity of the oil samples increased as the concentration of nanoparticles increased. The flash point and fire point of CMO are less than that of NCO and the blend samples.

Investigating the AW properties of the samples

Figures 1 and 2 show the variation of frictional coefficient and wear scar diameter of the lubricant oils under study, i.e. commercial mineral oil, blends of CNSL+NCO and r-GO additivated samples of 40% CNSL + NCO blends. From Figure 1, it can be apparently seen that all the values of friction coefficient and wear scar diameter of CNSL + NCO blend samples are significantly lower than those obtained for CMO samples.

The lowest friction coefficient among the blend samples was found for 40% CNSL+NCO sample, and this concentration was used for r-GO additivation at different concentrations. Figure 2 depicts the comparison between the r-GO additivated optimum blend samples against CMO, and it can be reasonably stated that the least coefficient of friction value was obtained at 0.5% r-GO + 40% CNSL + NCO sample which was less than the frictional coefficient value of CMO (0.105), while the least WSD was found at 1.0% of r-GO in the oil mixture.

It can also be seen that the optimum content of r-GO friction modifier in the biodegradable mixture of CNSL and NCO comprised between 0.5 and 1.0%. It was seen that the supplementary addition of r-GO up to 1.0% is beneficial, protecting the mating surfaces from direct contact. For reasons of economy in the following tests, the 0.5% r-GO + 40% CNSL + NCO sample was considered.

Analysis of extreme pressure properties of oil samples

The EP tests of CMO, 40% CNSL+NCO and 0.5% r-GO+40% CNSL+NCO samples are shown in the Figure 3.

As it can be depicted from the graphs, the LNSL and ISL values of the CMO were found to be superior to rest of the samples, but the weld load was 1260 N for all lubricant samples. The LNSL and ISL values

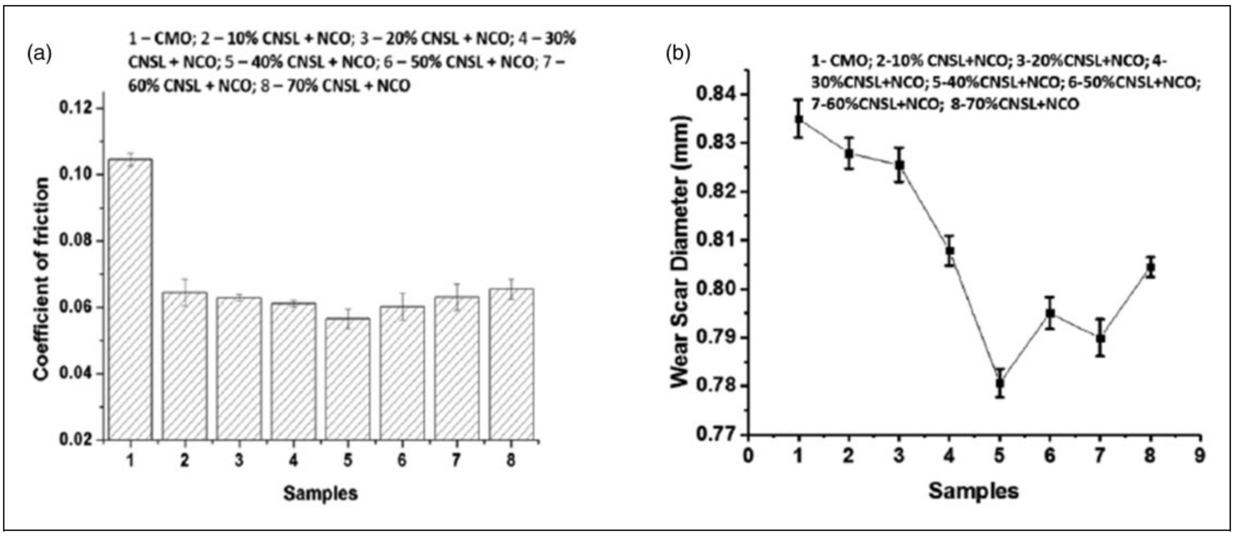

Figure 1. Variation of the friction coefficient (a), and wear scar diameter (b), for commercial mineral oil and samples of different percentages of CNSL + NCO blends.
CNSL: cashew nut shell liquid; NCO: neat castor oil.

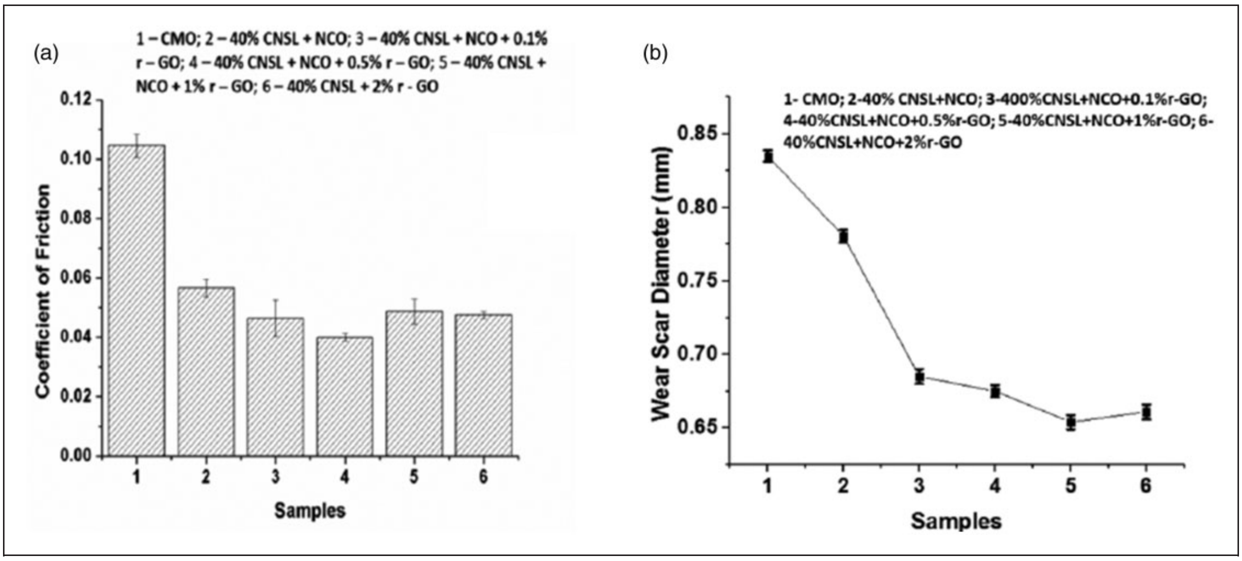

Figure 2. Variation of the friction coefficient (a), and wear scar diameter (b), for commercial mineral oil and samples of different percentages of r-GO in 40% CNSL + NCO + r-GO blends.
CNSL: cashew nut shell liquid; NCO: neat castor oil.

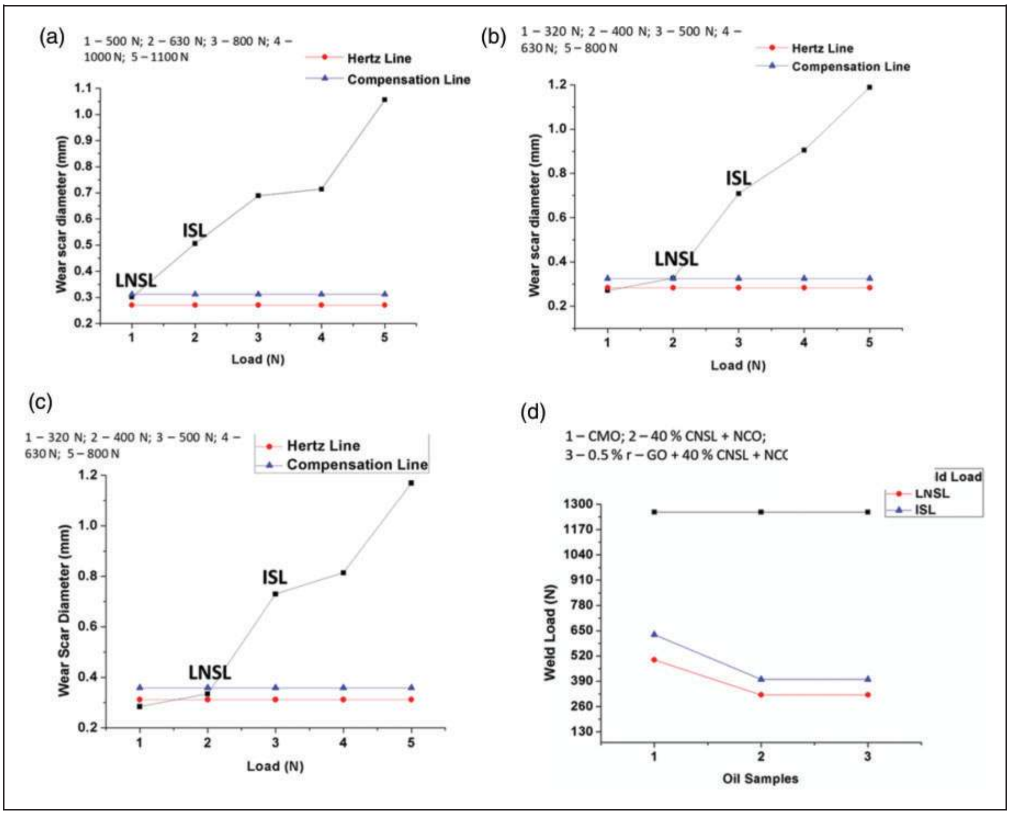

Figure 3. Wear scar diameter vs. load curve for: (a) CMO; (b) 40% CNSL + NCO; (c) 0.5% r-GO + 40% CNSL + NCO; (d) LNSL, ISL and WL of oil samples.

of CMO sample were found to be 500 N and 630 N, whereas the values for 40% CNSL+NCO sample and 0.5% r-GO+40% CNSL+NCO sample were 320 N and 400 N. The superior EP properties of CMO were due to the presence of the well-known EP additives: sulphur and phosphorus which were not present in NCO and CNSL samples.

Analysis of surface roughness of steel balls after the test

The SR of the scar surfaces of the balls treated with CMO, NCO, 40% CNSL + NCO and 0.5% r-GO+40% CNSL+NCO was examined using a three-dimensional profilometer after conducting anti-wear tests. As observed from Figure 4, the SR of CMO (Ra: 3.692 µm; Rq: 2.809 µm) sample is substantially higher as compared to NCO (Ra: 2.157 µm; Rq: 1.708 µm), 40% CNSL+NCO (Ra: 1.583 µm; Rq: 2.782 µm) and 0.5% r-GO + 40% CNSL+NCO (Ra: 1.150 µm; Rq: 2.046 µm) samples.

The results on SRs are in agreement with those obtained from anti-wear properties investigations (Figures 1 and 2), indicating that the metal-to-metal contact at the tribo-surface was high in the case of CMO than in the rest of the samples. Thus, the addition of r-GO as an additive further enhanced the performance of the finest blend CNSL-NCO concentration as compared to the values of CMO.

Discussion

Oil film thickness computation for EHD lubricated point contacts

The oil film thickness for Hertzian point contacts and EHD lubrication can be computed with the formulas of Hamrock and Dowson.[74–76] The oil film thickness in the center of the contact h_c and the minimum film thickness h_m are calculated according to equations (1) and (2), respectively.

$$h_c = 2.69 \cdot U^{0.67} \cdot G^{0.53} \cdot W^{-0.067} \cdot \left(1 - 0.61 \cdot e^{-0.73 \cdot k^*}\right) \cdot R_y \tag{1}$$

$$h_m = 3.63 \cdot U^{0.68} \cdot G^{0.49} \cdot W^{-0.073} \cdot \left(1 - e^{-0.68 \cdot k^*}\right) \cdot R_y \tag{2}$$

U, G and Z are non-dimensional parameters of speed, material and load, given by equations (3) to (5).

$$U = \frac{\eta_0 u_r}{E_0 R_y} \tag{3}$$

$$G = \alpha' E_0 \tag{4}$$

$$Z = \frac{Q}{E_o R_y^2} \tag{5}$$

η_0 = coefficient of dynamic viscosity of lubricant at the working temperature, in (Pa·s)

$$u_r = \frac{1}{2}(V_1 + V_2) \tag{6}$$

is the rolling speed in contact, and V_1, V_2 are the tangential speeds on the contacting bodies 1 and 2;

E_0 = equivalent Young's modulus (2.28 × 1011 Pa for steel on steel contacts)

$$E_0 = \frac{2}{\frac{(1-\nu_1^2)}{E1} + \frac{(1-\nu_2^2)}{E2}} \tag{7}$$

"ν" being the Poisson ratio and Indexes 1 and 2 refer to the contact bodies 1 and 2, respectively.

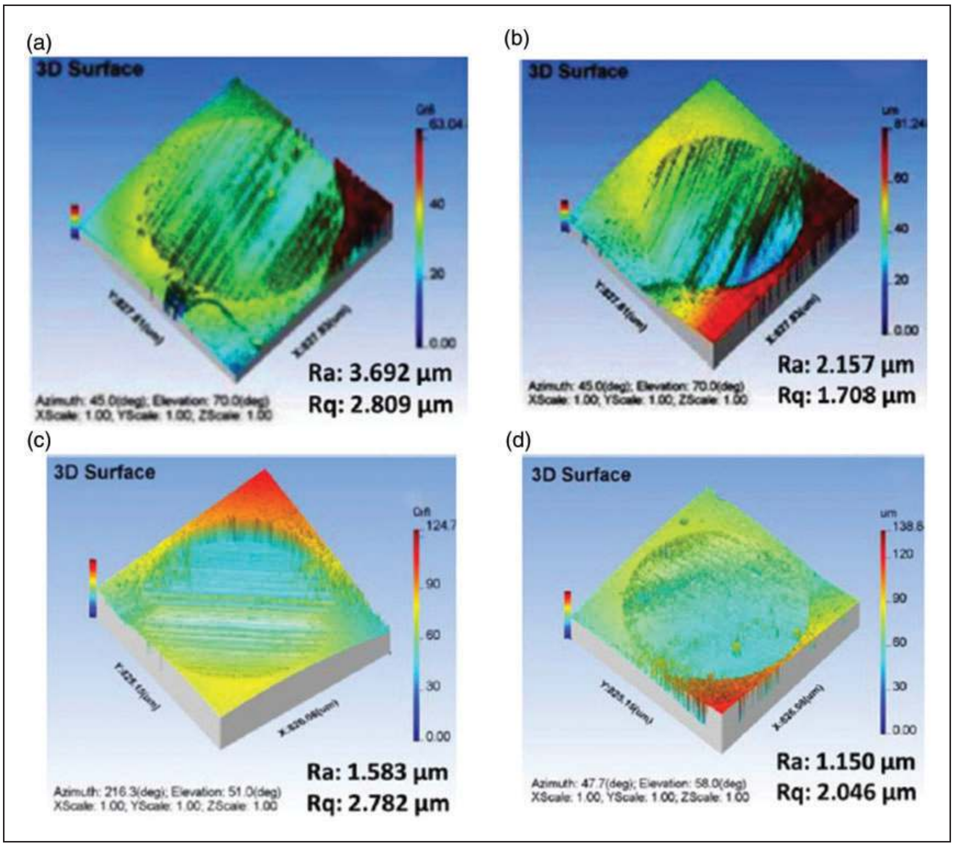

Figure 4. Profilometer images of WSD, (a) CMO; (b) NCO; (c) 40% CNSL + NCO; (d) 0.5% r-GO + 40% CNSL + NCO.

Ry = equivalent radius of contact bodies on rolling/sliding direction;

The coefficient of piezo-viscosity of lubricant, α', can be computed with Brüser relationship.[77]

$$\alpha' = \frac{0.0129.\ln(10^4.\eta)}{P_H^{0.25}}(\mathrm{MPa}^{-1}) \tag{8}$$

where η and PH represent the dynamic viscosity in Pa·s and Hertz pressure in (MPa), respectively.

$$k^* = 1.034\left(\frac{R_z}{R_y}\right)^{0.64} \tag{9}$$

For circular contact, the equivalent radius $R_z = R_y$, and $k^* = 1.034$, y is the rolling/sliding direction and z is the transversal direction to y.

For ball on ball contact of equal radius, $R_w = D_w/2$, D_w is the ball diameter, we get

$$R_y = R_x = D_w/4 \tag{10}$$

Q is the contact load. For the for ball machine arrangement (a pyramid formed by the upper ball on the three lower balls), Q is given by relationship shown in Equation 11.

$$Q = F_a/3\cos\theta \tag{11}$$

F_a is the axial load and θ is the angle between the directions of axial load F_a and normal load Q;

$$\theta = \sin^{-1}\left(\sqrt{3}/3\right) \tag{12}$$

The variation of the viscosity versus temperature and pressure is computed considering the Roelands – Barus model.[78] The Barus formula is

$$\eta(p, T) = \eta_0(T).\exp(\alpha'.P_H) \tag{13}$$

where $\eta_0(T)$is given by the Roelands formula as shown

$$\eta_o(T) = \left(10^{10^{\log(E)-B\log\left(1+\frac{T}{135}\right)}}\right) - 4.2 \tag{14}$$

Table 3 presents the values of central and minimum film thickness for all the sample oils, at the same load and speed. Neither the densities nor the viscosities of the blends modify too much with the addition of r-GO in small quantities (0.5, 1 and 2%). Analyzing the results from Table 3, it can be concluded that the addition of r-GO in small quantities insignificantly affects the oil film thickness computed with rheological classic formulas. Therefore, the action of the r-GO on the friction and wear must be explained considering the complex mechanisms of wear of surfaces and the interaction of various elements of hybrid lubricant on tribo pairs.

Wear mechanism between the tribo pairs

In order to comprehend the obtained results, the study of wear mechanism between the bodies in contact is imperative. The presence of saturated and unsaturated fatty acids in NCO as well as CNSL, as stated in Table 1, played consequential roles in the improvement of tribological properties, as they possessed an unprecedented molecular chain structure which influenced both friction and wear. As illustrated in Figure 5, the molecular structure of

Table 3. Oil film thickness and lubrication parameters for axial load of 392 N (maximum Hertz pressure = 3.423 GPa), speed 1200 r/min.

Oil sample	Density (g/cc)	Viscosity @40 °C (cSt)	Viscosity @ 100 °C (cSt)	Central oil film thickness (nm)	Minimum oil film thickness (nm)	Lambda parameter	α_p (Pa^{-1})
CMO	0.829	559.60	48.8	77	47	0.82 (boundary to mixed lubrication)	1.178×10^{-8}
NCO	0.925	242.81	18.10	41	24	0.44 (boundary lubrication)	1.046×10^{-8}
CNSL	0.880	65.03	8.04	18.2	10.5	0.193 (boundary lubrication)	8.657×10^{-9}
40% CNSL + NCO	0.907	215.61	17.99	39	23	0.415 (boundary lubrication)	1.034×10^{-8}
0.5% r-GO + 40% CNSL + NCO	0.912	198.58	16.78	37.04	21.40	0.393 (boundary lubrication)	1.022×10^{-8}
1% r-GO + 40% CNSL + NCO	0.916	205.8	16.4	37.14	21.46	0.394 (boundary lubrication)	1.023×10^{-8}
2% r-GO + 40% CNSL + NCO	0.925	208.26	16.67	37.85	21.87	0.402 (boundary lubrication)	1.027×10^{-8}

CMO: commercial mineral oil; NCO: neat castor oil; CNSL: cashew nut shell liquid; r-GO: reduced graphene oxide.

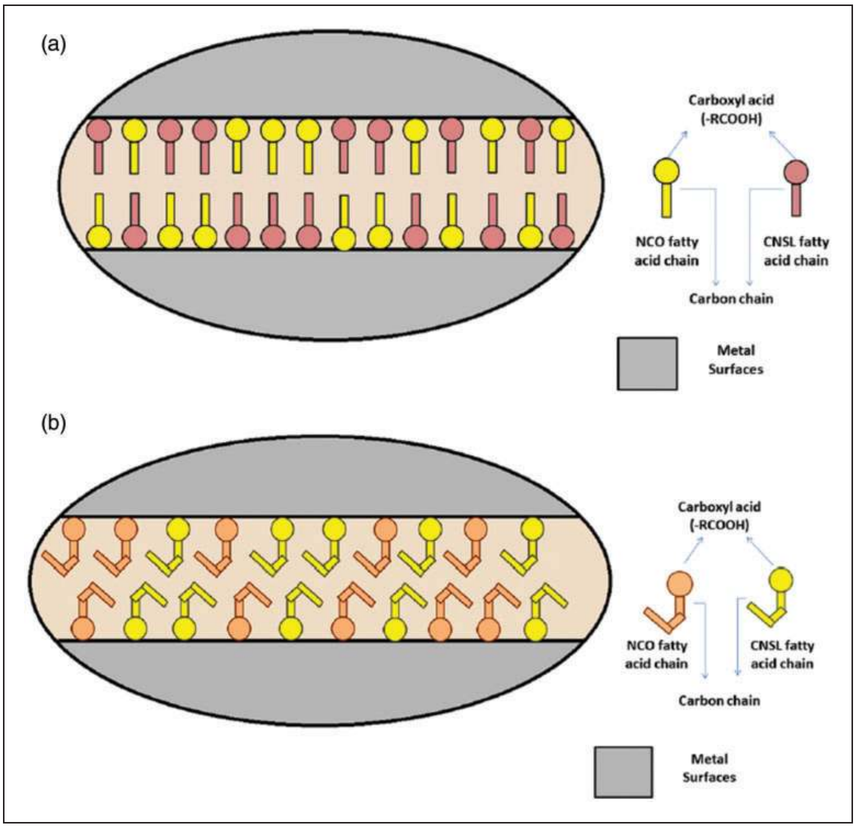

Figure 5. Structure of fatty acids in vegetable oils influencing friction and wear; (a) saturated chain; (b) unsaturated chain. CNSL: cashew nut shell liquid; NCO: neat castor oil.

saturated and unsaturated fatty acids was profoundly distinctive from each other. A saturated fatty acid chain, linear in nature contained a polar group of a hydrophobic carboxyl acid (–OH) that adhered to the metal surface on which it was acted upon. The nature of the linear chain impelled a parallel arrangement on the metal surfaces which furnished a smooth interaction during their relative motion between each other. A metal-to-metal contact happened due to the voids in between the molecules. An unsaturated fatty acid chain bent in nature contained a similar hydrophobic polar group which catered the reason for less surfaces in contact. The bent carbon chains did not provide much area for gaps between the molecules and resulted in less wear, although it provided a higher motion resistance and unsmooth interaction.[31]

The enhancement in frictional properties of the blended lubricants was boosted due to the presence of reduced graphene oxide as a frictional modifier.[31] Figure 6 illustrates as how the r-GO formed a tribo film on metal surfaces to reduce the friction and wear. The alkyl hydrophilic polar groups of r-GO assisted the molecule to keep it dispersed in oil, whereas the ester and triazole hydrophobic polar groups attached to the metal surfaces tribo-chemically (physisorption) reacting with them and thus forming a protective film on the metal surface.[79] Due to the unique geometry of the molecular structure of r-GO, they conduced to a high-surface film forming efficiency.[80] As it was interpreted from the results that a lower concentration of r-GO (0.1%) dispersed easily in oil and lubricated the surface although in this concentration, it was difficult to form a stable layer all over the contact area. The uncovered surfaces slided over each other and caused friction which contributed to a low reduction in coefficient of friction. The higher concentration of r-GO (2%) contributed to a high coefficient of friction as well as r-GO filled up all the spaces on the metal surface till the point of saturation and the residual unfilled particles formed debris which led to abrasive-like wear.[31] Thus, an optimum r-GO particle concentration provided the highest reduction in friction coefficient.

The expression of oil film thickness was used to express the film thickness of the lubricant beyond which the lubricant failed under given condition. This oil film strength (OFS)[81] can be calculated as given in equation (15)

$$\mathrm{OFS} = \frac{0.408\ (\text{axial load})}{\text{mean area of the wear scar}} \tag{15}$$

As seen from Figures 7 and 8, the optimum concentration of the blend and additives consisting of 40% wt. CNSL + NCO and 1.0% r-GO + 40% CNSL + NCO had the highest oil film strength.[45] It was observed that as CNSL concentration in the

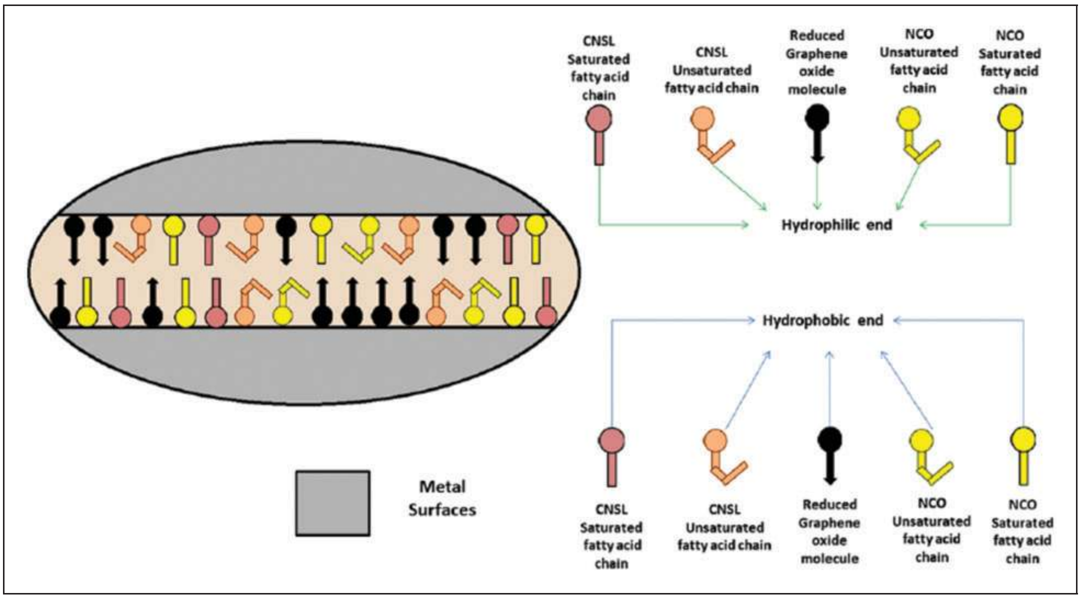

Figure 6. Interaction of various elements of hybrid lubricant on tribo pairs.
CNSL: cashew nut shell liquid; NCO: neat castor oil.

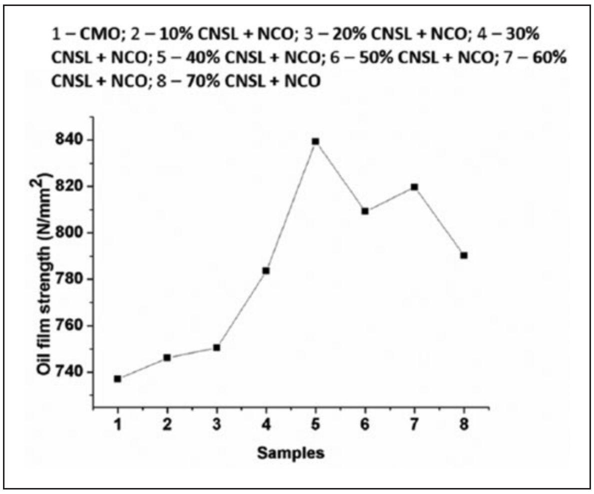

Figure 7. Oil film strength of CMO against different CNSL + NCO blends.
CNSL: cashew nut shell liquid; NCO: neat castor oil.

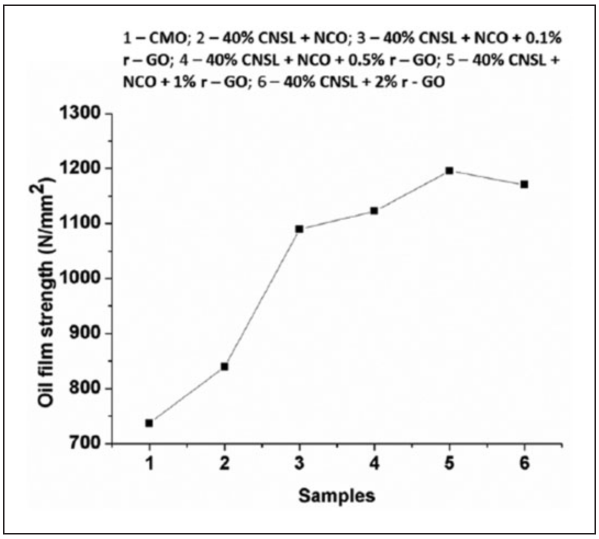

Figure 8. Oil film strength of CMO against 40% CNSL + NCO additivated with r-GO.
CNSL: cashew nut shell liquid; NCO: neat castor oil; r-GO: reduced graphene oxide.

blend increased, the value of oil film strength also increased. As the test conditions were related to elevated temperatures and sliding of the metal surfaces over each other, it was plausible that the saturated and unsaturated fatty acids of both the vegetable oils were oxidized, which were further accelerated with the formation of hexonic acids near the area of contact. Lubrication parameter values presented in Table 3 indicated mixed and boundary lubrication conditions. Accordingly, the SEM images of the wear scar (Figure 9(a) and (c)) showed normal scratches due to mild abrasion mechanism, without signs of deep furrows. However, minute particles were seen adhered to the surfaces on the wear track. Further to that the EDS results (Figure 9(b) and (d)) showed the oxygen in the r-GO and fatty acids of base oils might initiate reactions between the fatty acids of the NCO and CNSL oils and the tribo-surfaces, forming a protective oxide layer. The wear track of NCO+CNSL + r-GO was characterized using a micro Raman spectrograph (Figure 9(e)). The peaks at 387 cm^{-1} and 1276 cm^{-1} indicated the presence of hexanoic acid[82] on the steel surfaces from the degradation of vegetable oils. The presence of peaks at 452 cm^{-1} and 1586 cm^{-1} indicated the formation of secondary oxides such as iron oxide[83,84] and a tribo protection film by r-GO.[85] These stable films prevented metal to metal contact by furnishing a superior

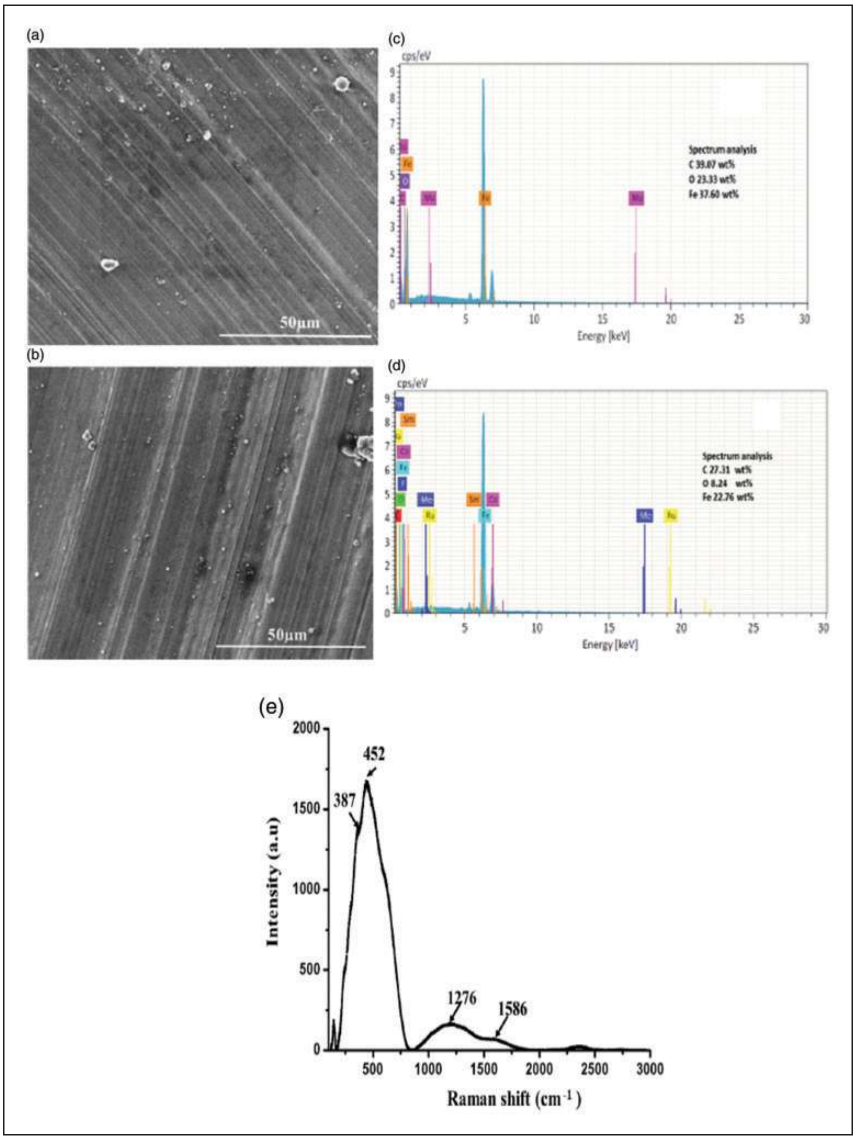

Figure 9. Scanning electron microscope images and EDS of the wear tracks on the balls tested with (a, b) NCO + 40% CNSL, (c, d) NCO + 40% CNSL + 0.5 wt% r-GO, (e) Raman spectrograph of the wear track in case of NCO + 40% CNSL + 0.5 wt% r-GO.

contact film over the asperities at the contact surface. The protective film between two surfaces augmented the tribological properties of the r-GO additived biodegradable oil.

Using the proposed blend of oil samples in a gear box

As seen from previous sections, NCO + CNSL + r-GO have shown excellent tribological properties as compared to commercial mineral oil. In order to practically prove the abilities of tested lubricants to cope with real applications, they were used in an in-house built gear box assembly (Figure 10). The gears (gear and pinion) were made of AISI 52100 steel with hardness of 55-58 Rc. A 1 Horsepower motor was used to drive the gears. The schematic diagram of the gear rig is shown in Figure 10(a). Initially, the machine was run at 350 rev/min for 1 h and 500 rev/min for next 51 1 h. The first 1 h was considered as running in period

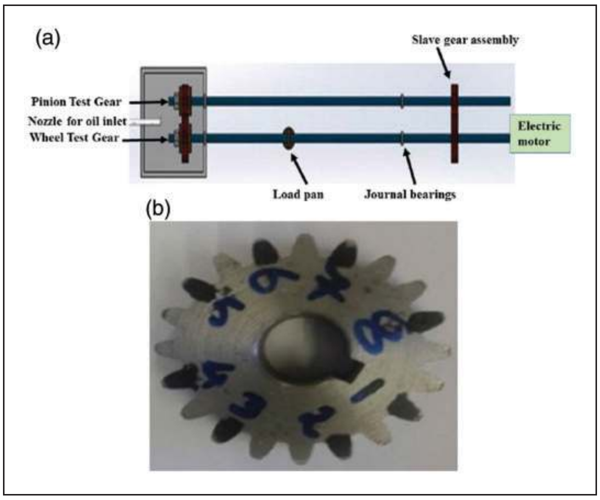

Figure 10. (a) Schematic diagram of the in-house build gear test rig, (b) one of the Spur gears (pinion) used in the test rig at test end.

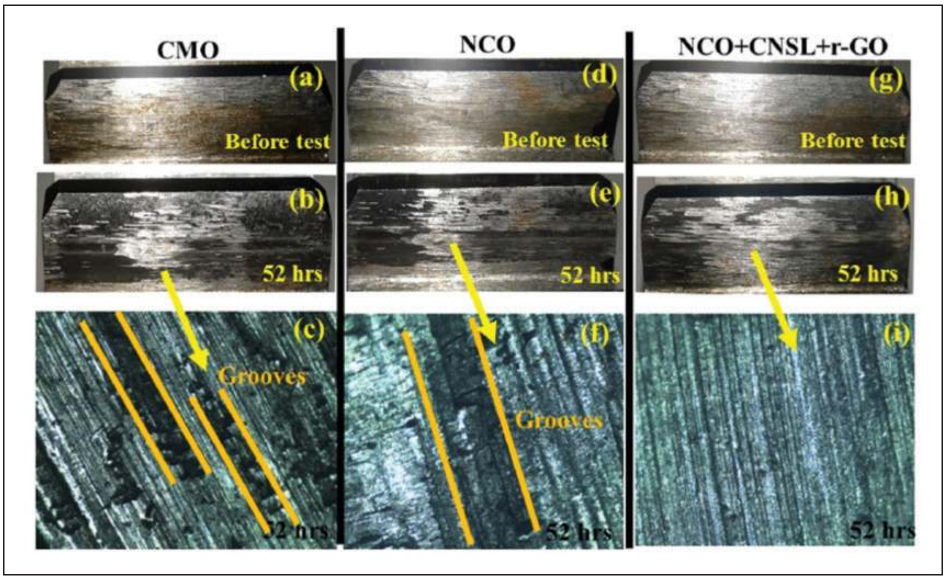

Figure 11. (a) Gear flank in CMO before test, (b) pictograph of gear teeth with CMO after 52 h, (c) optical microscope images of the gear teeth flank showing surface texture in CMO, (d) gear flank in NCO before test, (e) pictograph of gear teeth with NCO after 52 h (f) optical microscope images of the gear teeth flank showing the surface texture in NCO, (g) gear flank in NCO+CNSL + 0.5 wt% r-GO before test, (h) pictograph of gear teeth with NCO+CNSL + 0.5 wt% r-GO after 52 h, (i) optical microscope images of the gear teeth flank showing the surface texture in NCO+CNSL + 0.5 wt% r-GO.
CNSL: cashew nut shell liquid; NCO: neat castor oil; r-GO: reduced graphene oxide.

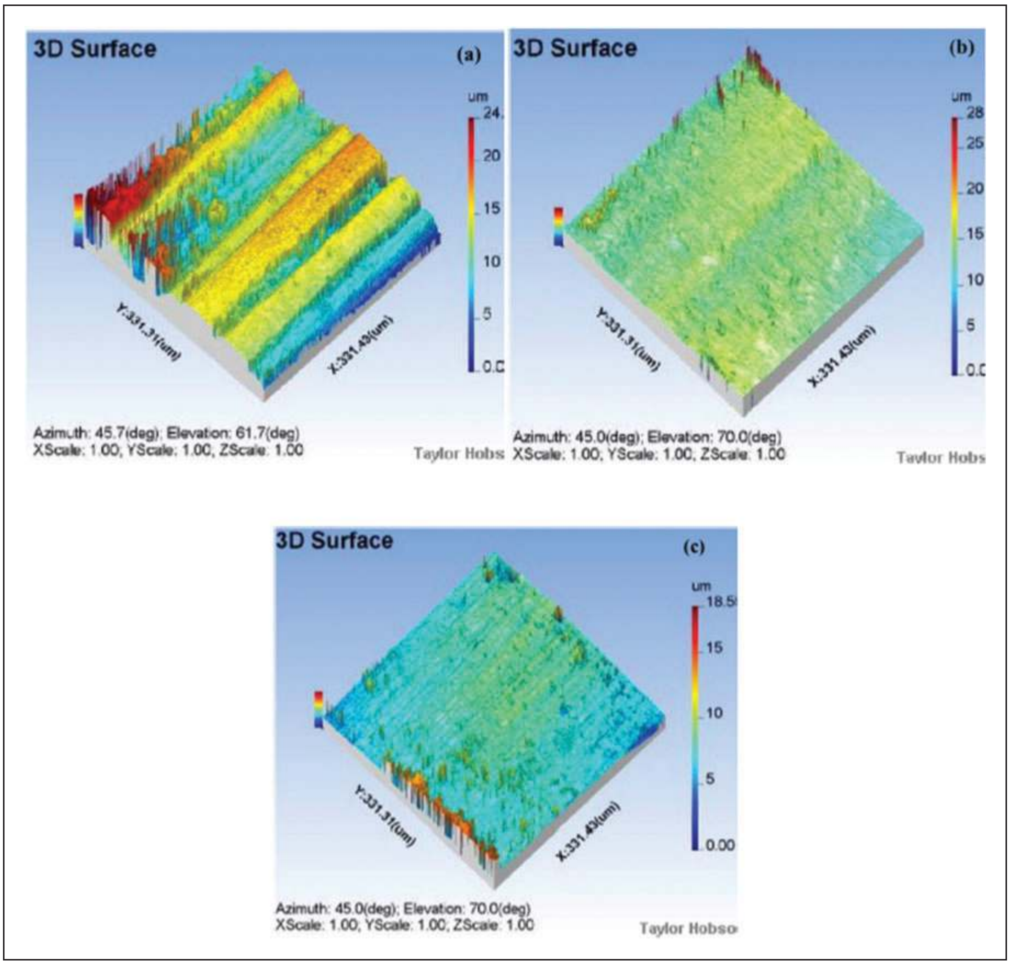

Figure 12. Three dimensional images of the gear flanks after 52 h with (a) CMO; (b) NCO; (c) NCO + 40% CNSL + 0.5 wt% r-GO.

to achieve maximum contact between the gears, and the later 51 h were considered as operation period. Some teeth of the pinion were marked as shown in Figure 10(b) and those teeth were observed closely. A spray type lubricant disperser was used to lubricate the gears. The lubricant spray time was adjusted for 3 s with an interval of 8 s. Such an arrangement is found in open gear systems. The gears were loaded at 140 N. Figure 11 shows the surfaces of the gear teeth that ran with CMO, NCO and NCO + CNSL + 0.5 wt% r-GO for 52 h.

From Figures 11 and 12, it can be seen that the gear which ran with CMO had shown more damaged surfaces as compared to NCO. The gear flank surface in case of NCO + 40% CNSL + 0.5 wt% r-GO did not show any sign of damage. There was not much difference in the roughness values of the undamaged gear teeth with all the oil samples, as the roughness of the teeth varied between 0.160 µm and 0.434 µm. The only concern was that grooves started on almost all the teeth of the gears which was running with CMO, followed by NCO but normal sliding marks were seen in the teeth with NCO + 40% CNSL + 0.5 wt% r-GO. These observations are in line with the laboratory results previously presented in this paper. Thus, it can be said that the bend of NCO + 40% CNSL + 0.5 wt% r-GO exhibited better lubricating properties than CMO and NCO, and hence showing that a green and clean lubricant shows competitive performance when compared to a non-biodegradable lubricant.

Conclusions

The present investigation focused on the optimisation of the percentage of CNSL, NCO and r-GO friction modifier in a new biodegradable lubricating mixture. With this aim, tests on a four-ball machine were carried out. The tribological properties such as coefficient of friction, wear scar diameter, roughness and surface analysis for the NCO-based lubricant blended with CNSL in varying proportions were studied. The optimum concentration of CNSL in the castor oil is 40%. The previous obtained biodegradable blend of oils was treated with different weight percentages (0.1% to 2%) of r-GO nanoparticles, to determine the best lubricating mixture from the viewpoint of anti-wear properties. The performances of the new biodegradable oil and r-GO mixture were compared against those of CMO containing phosphorus (4 ppm) and sulphur (4977 ppm). One of the prime properties of CMO is to have a low frictional coefficient. The coefficient of friction (CoF), in the case of 40% CNSL + NCO (CoF: 0.0565) and 0.5% r-GO + 40% CNSL + NCO (CoF: 0.0399) was significantly less than that of CMO (CoF: 0.1044). The performance of 40% CNSL + NCO was 45.8% better than CMO, and the performance of 0.5% r-GO + 40% CNSL + NCO was found to be 61.7% better than CMO. The wear scar diameters of CNSL + NCO blend samples and r-GO additivated blend samples were found to be less than CMO. The wear scar diameter in case of 1% r-GO was found to be the lowest. It can be clearly concluded that energy consumption in case of the vegetable oil samples would be less than that of CMO. The oil film strength of 40% CNSL + NCO oil sample was found to be highest among all CNSL + NCO blends, and 1.0% r-GO + 40% CNSL + NCO sample had the highest oil film strength as compared to other concentrations of additives in the oil mixture. The three-dimensional surface roughness shows that the roughness Ra of 0.5% r-GO + 40% CNSL + NCO sample (1.150 µm) was lesser than that of 40% CNSL + NCO sample (1.583 µm). The surface characteristics of both the samples were found to be superior to CMO and NCO samples. According to the previous presented results, r-GO is found to be a promising nano-friction modifier in CNSL + NCO blends. The physical and chemical mechanisms taking place within the tribo-contacts lubricated by r-GO additivated biodegradable mixture were thoroughly explained on the base of SEM, EDS, and surface topography analysis.

Finally, the new biodegradable mixture, the non-biodegradable CMO, and a NCO are implemented as lubricants in a gearbox, the long tests proved the superiority of the biodegradable mixture. The preliminary results of the present work proved that the new biodegradable CNSL–NCO mixture, proper additivated with r-GO friction modifier, can successfully replace the CMOs in various applications. The usage of additivated vegetable oil blends as a possible replacement of CMO will pave the way for sustainable lubrication and green tribology. Future research must concentrate on increasing the extreme pressure performances of biodegradable lubricating mixture, by adding new environmentally friendly additives.

Acknowledgements

The authors are grateful to Mr. Rishabh Maggirwar, SRM Institute of Science and Technology who helped in conducting the experiments.

Declaration of Conflicting Interests

The author(s) declared no potential conflicts of interest with respect to the research, authorship, and/or publication of this article.

Funding

The author(s) disclosed receipt of the following financial support for the research, authorship, and/or publication of this article: The authors acknowledge the financial support from Science and Engineering Research Board, Department of Science and Technology, India under Teachers Associateship for Research Excellence (TARE) scheme (File No. TAR/2018/000202).

ORCID iD

Shubrajit Bhaumik https://orcid.org/0000-0001-6803-4387

References

1. Wang Y, Li C, Zhang Y, et al. Comparative evaluation of the lubricating properties of vegetable-oil-based nanofluids between frictional test and grinding experiment. *Manuf Process* 2007; 26: 94–104.
2. Imran A, Masjuki HH, Kalam MA, et al. Study of friction and wear characteristic of jatropha oil blended lube oil. *Procedia Eng* 2013; 68: 178–185.
3. Suhane A, Sarviya RM, Siddiqui AR, et al. Optimization of wear performance of castor oil based lubricant using Taguchi technique. *Mater Today: Proc* 2017; 4: 2095–2104.
4. Anand A, Irfan Ul Haq M, Vohra K, et al. Role of green tribology in sustainability of mechanical systems: a state of the art survey. *Mater Today: Proc* 2017; 4: 3659–3366.
5. Shahabuddin M, Masjuki H and Kalam M. Experimental investigation into tribological characteristics of bio-lubricant formulated from jatropha oil. *Procedia Eng* 2013; 56: 597–606.
6. Siniawski MT, Saniei N, Adhikari B, et al. Influence of fatty acid composition on the tribological performance of two vegetable based lubricants. *J Synth Lubr* 2007; 24: 101–110.
7. Bhaumik S, Pathak SD, Dey S, et al. Artificial intelligence based design of multiple friction modifiers dispersed castor oil and evaluating its tribological properties. *Tribol Int* 2019; 140: 106813.
8. Biresaw G and Erhan S. Solid lubricant formulations containing starch-soybean oil composites. *J Am Oil Chem' Soc* 2003; 79: 291–296.
9. Zulhanafi P, Syahrullail S and Faridzuan M. Tribological performance of palm kernel oil added with nanoparticle copper oxide using fourball tribotester. *J Teknol* 2017; 79: 4–7.
10. Shahabuddin Ahmmad M, Hassan M and Abul Kalam M. Comparative corrosion characteristics of automotive materials in Jatropha biodiesel. *Int J Green Energy* 2018; 15: 1–7.
11. Ruggiero A, D'Amato R, Merola M, et al. Tribological characterization of vegetal lubricants: comparative experimental investigation on *Jatropha curcas* L. oil, rapeseed methyl ester oil, hydrotreated rapeseed oil. *Tribol Int* 2017; 109: 529–540.
12. Singh Y, Farooq A, Raza A, et al. Sustainability of a non-edible vegetable oil based bio-lubricant for automotive applications: a review. *Process Safe Environ* 2017; 111: 701–713.
13. Syahir A, Zulkifli N, Masjuki H, et al. A review on bio-based lubricants and their applications. *J Clean Prod* 2017; 168: 997–1016.
14. Luna F, Cavalcante J, Silva F, et al. Studies on biodegradability of bio-based lubricants. *Tribol Int* 2015; 92: 301–306.
15. McNutt J and He Q. Development of biolubricants from vegetable oils via chemical modification. *J Ind Eng Chem* 2016; 36: 1–12.
16. Quinchia L, Delgado M, Valencia C, et al. Viscosity modification of different vegetable oils with EVA copolymer for lubricant applications. *Ind Crop Prod* 2010; 32: 607–612.
17. Mahadi M, Choudhury I, Azuddin M, et al. Use of boric acid powder aided vegetable oil lubricant in turning AISI 431 steel. *Procedia Eng* 2017; 184: 128–136.
18. Ramezani M and Schmid S. Bio-based lubricants for forming of magnesium. *J Manuf Process* 2015; 19: 112–117.
19. Bétron C, Cassagnau P and Bounor-Legaré V. Control of diffusion and exudation of vegetable oils in EPDM copolymers. *Eur Polym J* 2016; 82: 102–113.
20. Issariyakul T and Dalai A. Biodiesel from vegetable oils. *Renew Sust Energ Rev* 2014; 31: 446–471.
21. Sánchez R, Stringari G, Franco J, et al. Use of chitin, chitosan and acylated derivatives as thickener agents of vegetable oils for bio-lubricant applications. *Carbohydr Polym* 2011; 85: 705–714.
22. Reeves C, Siddaiah A and Menezes P. Tribological study of imidazolium and phosphonium ionic liquid-based lubricants as additives in carboxylic acid-based natural oil: advancements in environmentally friendly lubricants. *J Clean Prod* 2018; 176: 241–250.
23. Ionescu M, Radojčić D, Wan X, et al. Functionalized vegetable oils as precursors for polymers by thiol-ene reaction. *Carbohydr. Polym* 2015; 67: 439–448.
24. Paredes X, Comuñas M, Pensado A, et al. High pressure viscosity characterization of four vegetable and mineral hydraulic oils. *Ind Crop Prod* 2014; 54: 281–290.
25. Syahrullail S, Kamitani S and Shakirin A. Performance of vegetable oil as lubricant in extreme pressure condition. *Procedia Eng* 2013; 68: 172–177.
26. Cermak S, Biresaw G, Isbell T, et al. New crop oils – properties as potential lubricants. *Ind Crop Prod* 2013; 44: 232–239.
27. Reeves C, Menezes P, Jen T, et al. The influence of fatty acids on tribological and thermal properties of natural oils as sustainable biolubricants. *Tribol Int* 2015; 90: 123–134.
28. Martín-Alfonso J, López-Beltrán F, Valencia C, et al. Effect of an alkali treatment on the development of cellulose pulp-based gel-like dispersions in vegetable oil for use as lubricants. *Tribol Int* 2018; 123: 329–336.
29. Talib N and Rahim E. The effect of tribology behavior on machining performances when using bio-based lubricant as a sustainable metalworking fluid. *Procedia CIRP* 2016; 40: 504–508.
30. Arumugam S, Sriram G and Ellappan R. Bio-lubricant-biodiesel combination of rapeseed oil: an experimental investigation on engine oil tribology, performance, and emissions of variable compression engine. *Energy* 2014; 72: 618–627.
31. Bahari A, Lewis R and Slatter T. Friction and wear response of vegetable oils and their blends with mineral engine oil in a reciprocating sliding contact at severe contact conditions. *Proc Inst Mech Eng J* 2017; 232: 244–258.
32. Talib N and Rahim E. Performance of modified jatropha oil in combination with hexagonal boron nitride particles as a bio-based lubricant for green machining. *Tribol Int* 2018; 118: 89–104.
33. Ruggiero A, D'Amato R, Merola M, et al. On the tribological performance of vegetal lubricants: experimental investigation on *Jatropha curcas* L. oil. *Procedia Eng* 2016; 149: 431–437.
34. Boshui C, Kecheng G, Jianhua F, et al. Tribological characteristics of monodispersed cerium borate nanospheres in biodegradable rapeseed oil lubricant. *Appl Surf Sci* 2015; 353: 326–332.

35. Wang Z, Ren R, Song H, et al. Improved tribological properties of the synthesized copper/carbon nanotube nanocomposites for rapeseed oil-based additives. *Appl Surf Sci* 2018; 428: 630–639.
36. Jayadas N, Prabhakaran Nair K and Ajithkumar G. Tribological evaluation of coconut oil as an environment-friendly lubricant. *Tribol Int* 2007; 40: 350–354.
37. Koshy C, Rajendrakumar P and Thottackkad M. Evaluation of the tribological and thermo-physical properties of coconut oil added with MoS2 nanoparticles at elevated temperatures. *Wear* 2015; 330: 288–308.
38. Sánchez M, Avhad M, Marchetti J, et al. Jojoba oil: a state of the art review and future prospects. *Energy Convers Manag* 2016; 129: 293–304.
39. Bouaid A, Bajo L, Martinez M, et al. Optimization of biodiesel production from jojoba oil. *Process Saf Environ* 2007; 85: 378–382.
40. Vedharaj S, Vallinayagam R, Yang W, et al. Synthesis and utilization of catalytically cracked cashew nut shell liquid in a diesel engine. *Exp Therm Fluid Sci* 2016; 70: 316–324.
41. Sanjeeva S, Pinto M, Narayanan M, et al. Distilled technical cashew nut shell liquid (DT-CNSL) as an effective biofuel and additive to stabilize triglyceride biofuels in diesel. *Renew Energ* 2014; 71: 81–88.
42. Menon ARR, Pillai CKS, Sudha JD, et al. Cashew nut shell liquid – its polymeric and other industrial products. *J Sci Ind Res* 1985; 44: 324–328.
43. Kasiraman G, Edwin Geo V and Nagalingam B. Assessment of cashew nut shell oil as an alternate fuel for CI (Compression ignition) engines. *Energy* 2016; 101: 402–410.
44. Bhaumik S, Datta S and Pathak S. Analyses of tribological properties of castor oil with various carbonaceous micro- and nano-friction modifiers. *J Tribol* 2017; 139: 061802.
45. Bhaumik S, Maggirwar R, Datta S, et al. Analyses of anti-wear and extreme pressure properties of castor oil with zinc oxide nano friction modifiers. *Appl Surf Sci* 2018; 449: 277–286.
46. Bhaumik S and Pathak SD. A comparative experimental analysis of tribological properties between commercial mineral oil and neat castor oil using Taguchi method in boundary lubrication regime. *Tribol Ind* 2016; 38: 33–44.
47. Martin JM, Matta C, Bouchet M, et al. Mechanism of friction reduction of unsaturated fatty acids as additives in diesel fuels. *Friction* 2013; 1: 252–258.
48. Ossia CV, Han HG and Kong H. Response surface methodology for eicosanoic acid tribo properties in castor oil. *Tribol Int* 2008; 42: 50–58.
49. Bhaumik S, Paleu V, Pathak R, et al. Tribological investigation of r-GO additived biodegradable cashew nut shells liquid as an alternative industry lubricant. *Tribol Int* 2019; 135: 500–509.
50. Suhane A, Sarviya RM, Rehman A, et al. Suitability of alternative lubricants for automotive gear applications. *Int J Eng Res Appl* 2014; 4: 64–67.
51. Abdul Khaliq R, Kafafy R, Salleh HM, et al. Enhancing the efficiency of polymerase chain reaction using graphene nanoflakes. *Nanotechnology* 2012; 23: 455106.
52. Rasheed A, Khalid M, Rashmi W, et al. Graphene based nanofluids and nanolubricants – review of recent developments. *Renew Sust Energ Rev* 2016; 63: 346–362.
53. Rasheed A, Khalid M, Javeed A, et al. Heat transfer and tribological performance of graphene nanolubricant in an internal combustion engine. *Tribol Int* 2016; 103: 504–515.
54. Quinchia L, Delgado M, Reddyhoff T, et al. Tribological studies of potential vegetable oil-based lubricants containing environmentally friendly viscosity modifiers. *Tribol Int* 2014; 69: 110–117.
55. Tang Z and Li S. A review of recent developments of friction modifiers for liquid lubricants (2007–present). *Curr Opin Solid St M* 2014; 18: 119–139.
56. Zareh-Desari B and Davoodi B. Assessing the lubrication performance of vegetable oil-based nano-lubricants for environmentally conscious metal forming processes. *J Clean Prod* 2016; 135: 1198–1209.
57. Shankar S, Praveenkumar G and Krishnakumar P. Experimental study on frictional characteristics of tungsten carbide versus carbon as mechanical seals under dry and eco-friendly lubrications. *Int J Refract Metals Hard Mater* 2016; 54: 39–45.
58. Guimarey M, Salgado M, Comuñas M, et al. Effect of ZrO_2 nanoparticles on thermophysical and rheological properties of three synthetic oils. *J Mol Liq* 2018; 262: 126–138.
59. Guzman Borda F, Ribeiro de Oliveira S, Seabra Monteiro Lazaro L, et al. Experimental investigation of the tribological behavior of lubricants with additive containing copper nanoparticles. *Tribol Int* 2018; 117: 52–58.
60. Berman D, Erdemir A and Sumant A. Graphene: a new emerging lubricant. *Mater Today* 2014; 17: 31–42.
61. Sandoz-Rosado E, Tertuliano O and Terrell E. An atomistic study of the abrasive wear and failure of graphene sheets when used as a solid lubricant and a comparison to diamond-like-carbon coatings. *Carbon* 2012; 50: 4078–4084.
62. Liang H, Bu Y, Zhang J, et al. Graphene Oxide film as solid lubricant. *ACS Appl Mater Inter* 2013; 5: 6369–6375.
63. Berman D, Erdemir A and Sumant A. Reduced wear and friction enabled by graphene layers on sliding steel surfaces in dry nitrogen. *Carbon* 2013; 59: 167–175.
64. Ismail N and Bagheri S. Highly oil-dispersed functionalized reduced graphene oxide nanosheets as lube oil friction modifier. *Mater Sci Eng B* 2017; 222: 34–42.
65. Sharma AK, Katiyar JK, Bhaumik S, et al. Influence of alumina/MWCNT hybrid nanoparticle additives on tribological properties of lubricants in turning operation. *Friction* 2019; 7: 153–168.
66. Kinoshita H, Nishina Y, Alias AA, et al. Tribological properties of monolayer graphene oxide sheets as water-based lubricant additives. *Carbon* 2014; 66: 720–723.
67. Zhang Q, Wu B, Song R, et al. Preparation, characterization and tribological properties of polyalphaolefin with magnetic reduced graphene oxide/Fe3O4Tribol Int 2020; 141: 105952.
68. Padgurskas J, Rukuiza R, Prosyčevas I, et al. Tribological properties of lubricant additives of Fe, Cu and Co nanoparticles. *Tribol Int* 2013; 60: 224–232.
69. Ali M, Xianjun H, Mai L, et al. Improving the tribological characteristics of piston ring assembly in

automotive engines using Al2O3 and TiO2 nanomaterials as nano-lubricant additives. *Tribol Int* 2016; 103: 540–554.

70. Kimura Y, Wakabayashi T, Okada K, et al. Boron nitride as a lubricant additive. *Wear* 1999; 232: 199–206.
71. Pawlak Z, Kaldonski T, Pai R, et al. A comparative study on the tribological behaviour of hexagonal boron nitride (h-BN) as lubricating micro-particles – an additive in porous sliding bearings for a car clutch. *Wear* 2009; 267: 1198–1202.
72. Demas N, Timofeeva E, Routbort J, et al. Tribological effects of BN and MoS2 nanoparticles added to polyalphaolefin oil in piston skirt/cylinder liner tests. *Tribol Lett* 2012; 47: 91–102.
73. Riedo E and Brune H. Young modulus dependence of nanoscopic friction coefficient in hard coatings. *Appl Phys Lett* 2003; 83: 1986–1988.
74. Hamrock BJ and Dowson D. Isothermal elastohydrodynamic lubrication of point contacts. Part I – theoretical formulation. *J Lubrication Tech* 1976; 98: 223–229.
75. Hamrock BJ and Dowson D. Isothermal elastohydrodynamic lubrication of point contacts. Part II – ellipticity parameter results. *J Lubrication Tech* 1976; 98: 375–383.
76. Hamrock BJ and Dowson D. Isothermal elastohydrodynamic lubrication of point contacts. Part III – fully flooded results. *J Lubr Tech* 1977; 99: 264–276.
77. Brüggemann H and Kollman FG. A numerical solution of the thermal elastohydrodynamic lubrication in an elliptical contact. *J Lubrication Tech* 1982; 104: 392–400.
78. Bercea M, Paleu V and Bercea I. Lubricant oils additivated with polymers in EHD contacts: Part 1. Rheological behavior. *Lubr Sci* 2004; 17: 1–24.
79. Simič R and Kalin M. Comparison of alcohol and fatty acid adsorption on hydrogenated DLC coatings studied by AFM and tribological tests. *Stroj Vestn Mech E* 2013; 59: 707–718.
80. Rudnick LR. *Lubricant additives: chemistry and applications*. Boca Raton: CRC Press, 2009.
81. Paleu V, Bercea I, Cretu S, et al. Lubricant oils additivated with polymers in EHD contacts: part 2. Tests using a four-ball machine. *Lubr Sci* 2005; 17: 173–184.
82. Jehlicka J, Edwards HGM and Culka A. Using portable Raman spectrometers for the identification of organic compounds at low temperatures and high altitudes: exobiological applications. *Phil Trans R Soc A* 2010; 368: 3109–3125.
83. Lee H, Park YK, Kim SJ, et al. Facile synthesis of iron oxide/graphene nano composites using liquid phase plasma method. *J. Nanosci Nanotechnol* 2016; 16: 4483–4486.
84. De Faria DLA, Silva AV and De Oliveira MT. Raman micro spectroscopy of some iron oxides and oxyhydroxides. *J Raman Spectrosc* 1997; 28: 873–878.
85. Wu JB, Lin ML, Cong X, et al. Raman spectroscopy of graphene based materials and its application in related devices. *Chem Soc Rev* 2018; 47: 1822–1873.